

# High-power, fiber-laser-pumped, picosecond optical parametric oscillator based on MgO:sPPLT

S. Chaitanya Kumar<sup>1,\*</sup> and M. Ebrahim-Zadeh<sup>1,2</sup>

<sup>1</sup>ICFO-Institut de Ciències Fotoniques, Mediterranean Technology Park, 08860 Castelldefels, Barcelona, Spain

<sup>2</sup>Institució Catalana de Recerca i Estudis Avançats (ICREA), Passeig Lluís Companys 23, Barcelona 08010, Spain

\*chaitanya.suddapalli@icfo.es

**Abstract:** We report a stable, high-power, mid-infrared synchronously-pumped optical parametric oscillator (SPOPO) based on MgO:sPPLT, pumped by a 1064 nm, picosecond Yb-fiber laser operating at a repetition rate of 81.1 MHz. The singly resonant SPOPO is tunable over 1531-1642 nm (111 nm) in the near-infrared signal and 3022-3488 nm (466 nm) in the mid-infrared idler, providing a total tuning range of 577 nm. Careful optimization of output coupling results in a signal output power as high as 4.3 W at 1593 nm and a mid-infrared idler power of 2 W at 3204 nm for 13.4 W of pump power at a total extraction efficiency of 47%. The SPOPO can be operated near room temperature, down to 30 °C, and exhibits passive peak-to-peak power stability better than 8.6% at 1568 nm (signal) and 8.2% at 3310 nm (idler) over 13 hours at full power. The output signal pulses have duration of 17.5 ps, with a FWHM spectral bandwidth of 1.4 nm centered at 1568 nm.

©2011 Optical Society of America

**OCIS codes:** (190.4360) Nonlinear optics, devices; (190.4400) Nonlinear optics, materials; (190.4970) Parametric oscillators and amplifiers; (190.2620) Harmonic generation and mixing.

---

## References and links

1. S. Chaitanya Kumar, R. Das, G. K. Samanta, and M. Ebrahim-Zadeh, "Optimally-output-coupled, 17.5 W, fiber-laser-pumped continuous-wave optical parametric oscillator," *Appl. Phys. B* **102**(1), 31–35 (2011).
2. T. P. Lamour, L. Kornaszewski, J. H. Sun, and D. T. Reid, "Yb: fiber-laser-pumped high-energy picosecond optical parametric oscillator," *Opt. Express* **17**(16), 14229–14234 (2009).
3. C. W. Freudiger, W. Min, B. G. Saar, S. Lu, G. R. Holtom, C. He, J. C. Tsai, J. X. Kang, and X. S. Xie, "Label-free biomedical imaging with high sensitivity by stimulated Raman scattering microscopy," *Science* **322**(5909), 1857–1861 (2008).
4. A. Baron, A. Rysanyanskiy, N. Dubreuil, P. Delaye, Q. Vy Tran, S. Combrié, A. de Rossi, R. Frey, and G. Roosen, "Light localization induced enhancement of third order nonlinearities in a GaAs photonic crystal waveguide," *Opt. Express* **17**(2), 552–557 (2009).
5. M. V. O'Connor, M. A. Watson, D. P. Shepherd, D. C. Hanna, J. H. V. Price, A. Malinowski, J. Nilsson, N. G. R. Broderick, D. J. Richardson, and L. Lefort, "Synchronously pumped optical parametric oscillator driven by a femtosecond mode-locked fiber laser," *Opt. Lett.* **27**(12), 1052–1054 (2002).
6. O. Kokabee, A. Esteban-Martin, and M. Ebrahim-Zadeh, "Efficient, high-power, ytterbium-fiber-laser-pumped picosecond optical parametric oscillator," *Opt. Lett.* **35**(19), 3210–3212 (2010).
7. S. C. Kumar, G. K. Samanta, and M. Ebrahim-Zadeh, "High-power, single-frequency, continuous-wave second-harmonic-generation of ytterbium fiber laser in PPKTP and MgO:sPPLT," *Opt. Express* **17**(16), 13711–13726 (2009).
8. G. K. Samanta, S. C. Kumar, K. Devi, and M. Ebrahim-Zadeh, "Multicrystal, continuous-wave, single-pass second-harmonic generation with 56% efficiency," *Opt. Lett.* **35**(20), 3513–3515 (2010).
9. S. Chaitanya Kumar and M. Ebrahim-Zadeh, "High-power, continuous-wave, mid-infrared optical parametric oscillator based on MgO:sPPLT," *Opt. Lett.* **36**(13), 2578–2580 (2011).
10. K. V. Bhupathiraju, J. D. Rowley, and F. Ganikhanov, "Efficient picosecond optical parametric oscillator based on periodically poled lithium tantalate," *Appl. Phys. Lett.* **95**(8), 081111 (2009).
11. K. V. Bhupathiraju, A. D. Seymour, and F. Ganikhanov, "Femtosecond optical parametric oscillator based on periodically poled stoichiometric LiTaO<sub>3</sub> crystal," *Opt. Lett.* **34**(14), 2093–2095 (2009).
12. J. D. Rowley, S. Yang, and F. Ganikhanov, "Power and tuning characteristics of a broadly tunable femtosecond optical parametric oscillator based on periodically poled stoichiometric lithium tantalate," *J. Opt. Soc. Am. B* **28**(5), 1026–1036 (2011).

13. T. Südmeyer, J. Aus der Au, R. Paschotta, U. Keller, P. G. R. Smith, G. W. Ross, and D. C. Hanna, "Femtosecond fiber-feedback optical parametric oscillator," *Opt. Lett.* **26**(5), 304–306 (2001).
14. T. Südmeyer, E. Innerhofer, F. Brunner, R. Paschotta, T. Usami, H. Ito, S. Kurimura, K. Kitamura, D. C. Hanna, and U. Keller, "High-power femtosecond fiber-feedback optical parametric oscillator based on periodically poled stoichiometric LiTaO<sub>3</sub>," *Opt. Lett.* **29**(10), 1111–1113 (2004).
15. H. Ishizuki and T. Taira, "High energy quasi-phase matched optical parametric oscillation using Mg-doped congruent LiTaO<sub>3</sub> crystal," *Opt. Express* **18**(1), 253–258 (2010).
16. T. Hatanaka, K. Nakamura, T. Taniuchi, H. Ito, Y. Furukawa, and K. Kitamura, "Quasi-phase-matched optical parametric oscillation with periodically poled stoichiometric LiTaO<sub>3</sub>," *Opt. Lett.* **25**(9), 651–653 (2000).
17. A. Bruner, D. Eger, M. B. Oron, P. Blau, M. Katz, and S. Ruschin, "Temperature-dependent Sellmeier equation for the refractive index of stoichiometric lithium tantalate," *Opt. Lett.* **28**(3), 194–196 (2003).
18. J. E. Bjorkholm, "Some effects of spatially nonuniform pumping in pulsed optical parametric oscillators," *IEEE J. Quantum Electron.* **7**(3), 109–118 (1971).
19. A. Esteban-Martin, O. Kokabee, and M. Ebrahim-Zadeh, "Optimum output coupling in optical oscillators using an antiresonant ring interferometer," *Opt. Lett.* **35**(16), 2786–2788 (2010).
20. S. Chaitanya Kumar, A. Esteban-Martin, and M. Ebrahim-Zadeh, "Interferometric output coupling of ring optical oscillators," *Opt. Lett.* **36**(7), 1068–1070 (2011).

## 1. Introduction

Recent advances in novel nonlinear materials and fiber laser pump sources have made optical parametric oscillators (OPOs) compact, robust and efficient tunable sources operating in various temporal regimes, from continuous wave (cw) [1] to ultrafast [2] time-scales. In particular, synchronously pumped OPOs (SPOPOs) in the picosecond regime have emerged as versatile high-power sources of ultrashort pulses in spectral regions inaccessible to mode-locked lasers, catering a variety of applications from biomedicine [3] to material characterization [4]. Traditionally, such high-power SPOPOs have relied on the well-established quasi-phase-matched (QPM) nonlinear material, periodically poled lithium niobate (PPLN), providing multi-watt output powers in the mid-infrared (mid-IR) [5,6]. However, the new nonlinear material, periodically poled stoichiometric lithium tantalate (MgO:sPPLT) with superior thermal properties [7] has proved itself as an attractive alternative for frequency conversion in spectral regions extending from the visible to mid-IR in the cw regime [8,9]. In spite of a lower effective nonlinear coefficient ( $d_{\text{eff}} \sim 9$  pm/V) than PPLN ( $d_{\text{eff}} \sim 16$  pm/V), better transmission of LiTaO<sub>3</sub> in the 3–4  $\mu\text{m}$  spectral range can also benefit high-power mid-IR OPOs irrespective of the operating time scale.

Earlier work on mid-IR OPOs based on LiTaO<sub>3</sub> include the generation of picosecond [10] and femtosecond [11,12] pulses from a SPOPO using PPsLT pumped by a Kerr lens mode-locked (KLM) Ti:sapphire laser. High-power femtosecond fiber-feedback OPOs based on PPLT [13] and PPsLT [14] pumped by mode-locked Yb:YAG thin-disk lasers have also been demonstrated. Further, a nanosecond OPO using PPsLT [15] and a high-energy OPO based on large-aperture MgO:sPPLT pumped by Q-switched Nd:YAG laser at 1064 nm [16] have been reported. Also, recently, we demonstrated a high-power, Yb-fiber laser pumped cw OPO using MgO:sPPLT [9]. To our knowledge, picosecond SPOPOs based on MgO:sPPLT pumped by a fiber laser at 1064 nm, for mid-IR generation, have not been previously investigated. It would thus be of great interest to explore the feasibility of using MgO:sPPLT in SPOPOs pumped at 1064 nm, for the generation of high-average-power picosecond mid-IR radiation. Moreover, fiber laser pumping makes the SPOPO architecture compact, efficient, and robust, with the potential for power scaling.

## 2. Experimental setup

The schematic of the experimental setup is similar to that used in our previous experiments [6]. The pump source is a mode-locked Yb-fiber laser (Fianium FP1060-20) providing up to 20 W of output power in 20 ps pulses at a repetition rate of 81.1 MHz. The laser has a double-peak spectrum and operates at 1064 nm with an FWHM bandwidth of 1.38 nm, which is well below the spectral acceptance bandwidth of  $>2.5$  nm for optical parametric generation in a 30-mm-long MgO:sPPLT crystal, as used in our experiment. The MgO:sPPLT crystal is 1-mm-thick with six gratings, ranging in period from  $\Lambda = 29.15$   $\mu\text{m}$  to 30.65  $\mu\text{m}$ , and is housed in an oven whose temperature can be controlled in steps of  $\pm 0.1$  °C. The SPOPO is configured in a

four-mirror standing-wave cavity comprising two plano-concave mirrors ( $r = 150$  mm), one plane mirror and an output coupler. All mirrors have high reflectivity ( $R > 99\%$ ) over  $1.3\text{--}1.9$   $\mu\text{m}$  and high transmission ( $T > 90\%$ ) over  $2.2\text{--}4$   $\mu\text{m}$ , ensuring singly resonant oscillation. The pump beam is focused to a beam waist radius of  $68$   $\mu\text{m}$  ( $\xi \sim 0.5$ ) at the center of the nonlinear crystal, with a corresponding signal beam waist radius of  $83$   $\mu\text{m}$  ( $b_p \sim b_s$ ). A dichroic mirror separates the generated idler from the pump, while the signal power is extracted from the output coupler (OC). The total round-trip optical length of the cavity is  $\sim 370$  cm, ensuring synchronization with the pump laser.

### 3. Wavelength tuning and extracted power

In order to characterize the SPOPO, we initially performed temperature tuning for two grating periods,  $\Lambda = 30.65$  and  $30.15$   $\mu\text{m}$ , by varying the crystal temperature. The signal wavelength was measured using a near-infrared spectrum analyzer and the corresponding idler wavelength was calculated from energy conservation. Figure 1 shows the measured output power across the tuning range of the picosecond MgO:sPPLT SPOPO with a maximum pump power of  $13.6$  W at the input to the crystal. In order to achieve signal power extraction across the full SPOPO tuning range, we deployed two OCs available in our laboratory. Figure 1(a) shows the extracted signal power with OC<sub>1</sub> ( $T \sim 10\%$  over  $1531\text{--}1568$  nm) and OC<sub>2</sub> ( $T \sim 25\text{--}70\%$  over  $1572\text{--}1642$  nm), together with the transmission of the OCs used to access the wide tuning range of the SPOPO. Using the two grating periods,  $\Lambda = 30.65$  and  $30.15$   $\mu\text{m}$ , and by changing

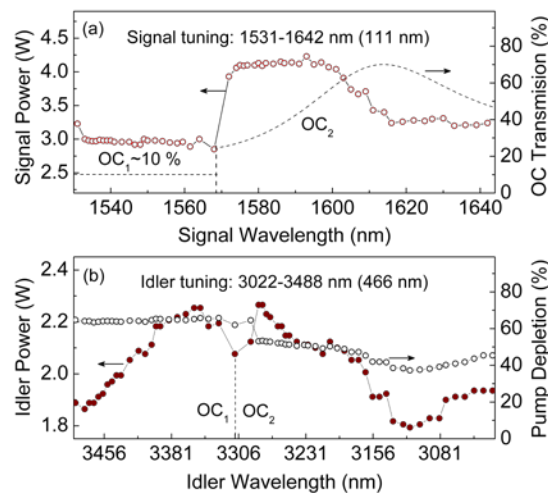


Fig. 1. Variation of (a) signal power together with transmission of different OCs, (b) idler power and pump depletion across the tuning range of MgO:sPPLT SPOPO.

the crystal temperature from  $30$   $^{\circ}\text{C}$  to  $200$   $^{\circ}\text{C}$ , we were able to tune the SPOPO over  $1531\text{--}1642$  nm in the signal and  $3022\text{--}3488$  nm in the idler wavelength range, resulting in a total (signal plus idler) tuning of  $577$  nm. We obtained good agreement between the theoretical temperature tuning curves calculated from the relevant Sellmeier equations [17] and the experimentally measured data. As shown in Fig. 1(a), the signal power extracted by deploying OC<sub>1</sub> is  $\sim 3$  W and is constant over the range  $1531\text{--}1568$  nm, implying that the output power is limited by the transmission of OC<sub>1</sub>. With OC<sub>2</sub>, the signal power varies from  $3.9$  W at  $1572$  nm to  $3.2$  W at  $1642$  nm, with maximum power obtained for an output coupling of  $27\text{--}60\%$ . It is interesting to note that the variation in the signal power in this output coupling range is nominal, indicating that the SPOPO is somewhat insensitive to losses. However, an overall comparison of the OC transmission and the extracted signal power shows that the variation of the signal power is not solely governed by the OC. The maximum signal power achieved was

4.2 W for an output coupling of ~47%. The corresponding idler power varies from 1.93 W at 3022 nm to 1.88 W at 3488 nm, with a maximum of 2.26 W at 3283 nm, as shown in Fig. 1(b), together with the pump depletion of >50% recorded over 61% of the idler tuning range.

#### 4. Power scaling and optimization

We also optimized the output coupling at a fixed signal wavelength, using  $\Lambda = 30.65 \mu\text{m}$ , by employing different OCs with signal transmission from T~5% to 88%. The measurements were performed at  $T = 100 \text{ }^\circ\text{C}$ , resulting in a signal wavelength of 1593 nm, corresponding to an idler wavelength of 3204 nm. Figure 2(a) shows the extracted signal power for different OCs at a maximum available input pump power of 13.3 W. Also shown in the inset of Fig. 2(a) is the simultaneously extracted idler power. As evident from the plot, an increase in the OC transmission from ~5% to ~47% resulted in an increase in the signal power from 2.4 W to 4.23 W, without significant compromise in the idler power remaining above 2 W. Further increase in the output coupling to 88% led to the drop in signal power down to 3.32 W, while the corresponding idler power decreased to 1.56 W. This implies an optimum signal output coupling of ~47% for our SPOPO at this wavelength, consistent with the data in Fig. 1 (a). For this value of optimum output coupling, the extraction efficiency is 46.9%, and the threshold pump power is recorded to be 2.8 W. Hence, the SPOPO is pumped ~4.8 times above threshold. This value is close the theoretical prediction for a Gaussian pump beam, where a maximum down-conversion efficiency of 71% is expected when pumping ~6.5 times above threshold [18]. In our SPOPO, the maximum pump depletion is >50% when pumping ~4.8 times threshold. One could adjust the output coupling so that the SPOPO is pumped at ~6.5 times above threshold, for the highest pump depletion. However, the focus of our study was the maximization of SPOPO output power and extraction efficiency. Further optimization of output coupling at different wavelengths across the SPOPO tuning range and for different pumping levels can be performed using interferometric techniques [19,20]. We also investigated power scaling of the SPOPO at the optimum output coupling, for  $\Lambda = 30.65 \mu\text{m}$ ,

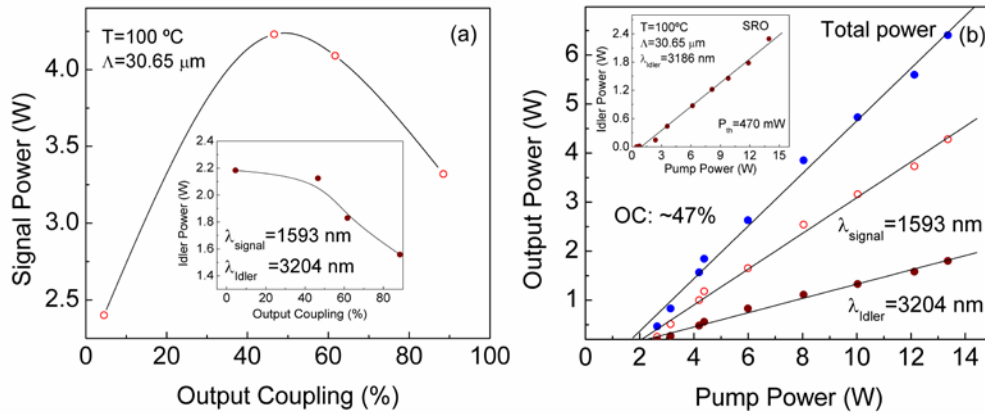


Fig. 2. (a) Variation of signal and (Inset) idler power from the picosecond MgO:sPPLT SPOPO as a function of output coupling for  $\Lambda = 30.65 \mu\text{m}$ . (b) Power scaling of the SPOPO at an optimum output coupling of ~47%. Inset: Power scaling in the absence of signal output coupling.

with the results shown in Fig. 2(b). In case of optimum output coupling of ~47%, we extracted as much as 4.28 W of signal power at 1593 nm, together with 2 W of mid-IR idler power at 3204 nm, for a pump power of 13.4 W, corresponding to a total power of 6.28 W, representing a total extraction efficiency of 46.9%, consistent with the measurements in Fig. 2(a). The threshold pump power for the optimally output-coupled SPOPO is 2.8 W, and the slope efficiencies of the extracted signal and idler power are 36.4% and 14.5%, respectively.

On the other hand, similar measurements for SPOPO with no output coupling resulted in a maximum idler power of 2.3 W at 3186 nm for a pump power of 13.9 W, as shown in the inset of Fig. 2(b), using the same grating period,  $\Lambda = 30.65 \mu\text{m}$ , at  $T = 100 \text{ }^\circ\text{C}$ . Under this condition, the SPOPO threshold pump power was as low as 470 mW. Also to be noted in Fig. 2(b) is the difference in the idler wavelengths when the SPOPO is operating with no output coupling (3186 nm) compared to that in the case of optimum output coupling (3204 nm). The corresponding signal wavelengths in the uncoupled and optimally output-coupled SPOPO are 1597 nm and 1593 nm, respectively. This difference in wavelength, despite SPOPO operating at the same temperature,  $T = 100 \text{ }^\circ\text{C}$  in both configurations, is attributed to the change in crystal temperature due to the small absorption at the signal wavelength due to significantly different intracavity power levels in the two configurations.

We also investigated the performance of the output-coupled SPOPO when operating close to room temperature. Figure 3 shows the variation of the signal, idler and total power as a function of pump power at  $T = 30 \text{ }^\circ\text{C}$  for a grating period of  $\Lambda = 30.15 \mu\text{m}$ , generating signal and idler wavelengths of 1531 nm and 3488 nm, respectively. These measurements were performed with a 10% OC, resulting in the extraction of 3.23 W of signal power at a slope efficiency of 25.8%, together with 1.86 W of mid-IR idler power at a slope efficiency of 15.3%, representing a total power of 5.09 W for a pump power of 13.7 W. The threshold of the SPOPO in this case was 1.87 W, owing to the 10% output coupling.

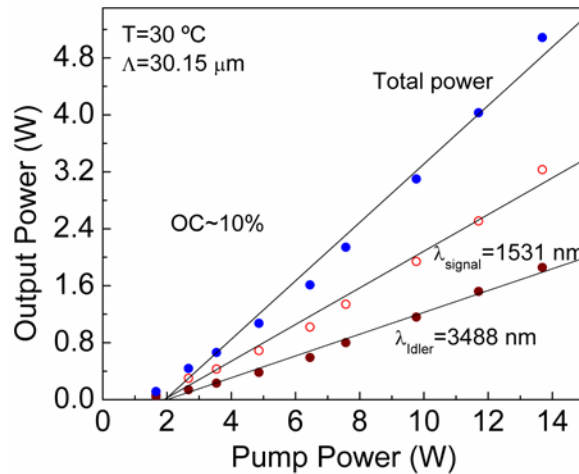


Fig. 3. Power scaling of picosecond MgO:sPPLT SPOPO using the  $\Lambda = 30.15 \mu\text{m}$  grating, with an output coupling of  $\sim 10\%$ .

Further, we compared the SPOPO performance at the same wavelength, while operating at different temperatures, by using two different grating periods. The high temperature operation of the SPOPO with  $\Lambda = 30.65 \mu\text{m}$  grating, was compared with the low temperature operation using  $\Lambda = 30.15 \mu\text{m}$  grating, generating the same signal and idler wavelengths. For example, at a temperature of  $170 \text{ }^\circ\text{C}$ , using a grating period of  $\Lambda = 30.15 \mu\text{m}$ , signal wavelength of 1572 nm, with a corresponding idler wavelength of 3273 nm, was generated. The extracted signal and idler powers under this condition were 3 W and 2.2 W, respectively, representing a total (signal plus idler) power of 5.2 W for an input pump power of 13.3 W. The same wavelengths can also be generated by using the grating period  $\Lambda = 30.65 \mu\text{m}$  and operating the SPOPO at a temperature of  $30 \text{ }^\circ\text{C}$ , close to room temperature. Under this condition, we were able to extract 3.9 W of signal together with 2.2 W of idler, representing a total power of 6.1 W for the same pump power. This confirms that the performance of the SPOPO is significantly better near room temperature than at high temperatures with regard to output power and extraction efficiency.

## 5. Power stability and temporal characterization

We recorded the long-term power stability of the picosecond MgO:sPPLT SPOPO close to room temperature, at  $T = 30\text{ }^{\circ}\text{C}$ , using OC<sub>2</sub> at a signal wavelength of 1568 nm, corresponding to mid-IR idler wavelength of 3310 nm, simultaneously at full output power. The result is shown in Fig. 4(a), where a peak-to-peak power stability of 8.6% for the signal and 8.2% for the idler over a period of 13 hours is obtained under free-running conditions. The long-term drift in the signal and idler power is due to the thermal and mechanical fluctuations effecting the cavity length and alignment of the SPOPO. However, realignment of the cavity at the end of the stability measurement resulted in the operation of the SPOPO with original performance. Hence, isolation from thermal and mechanical fluctuations will further improve the stability of the SPOPO [6].

Finally, we performed spectral and temporal characterization of the signal pulses from the picosecond MgO:sPPLT SPOPO. Figure 4(b) shows the typical interferometric autocorrelation, with signal pulse duration of  $\Delta\tau\sim 17.5\text{ ps}$ . The corresponding signal spectrum with a FWHM bandwidth of 1.4 nm, centered at 1568 nm, is shown in the inset of Fig. 4(b). These measurements correspond to a time-bandwidth product of  $\Delta\nu\Delta\tau\sim 3$  for the signal pulses, which can be further improved by implementing dispersion compensation.

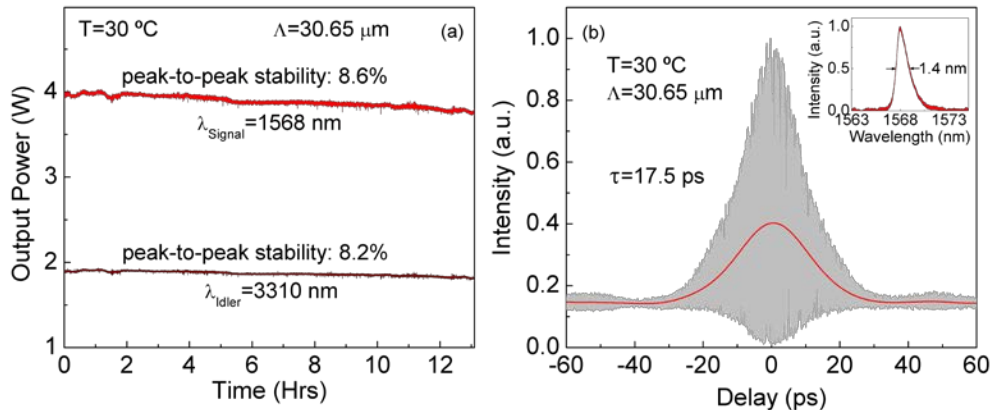


Fig. 4. (a) Long-term power stability of the signal and idler from the picosecond MgO:sPPLT SPOPO at  $T = 30\text{ }^{\circ}\text{C}$ . (b) Interferometric autocorrelation of the output signal pulses from the picosecond MgO:sPPLT SPOPO, and Inset: corresponding signal spectrum centered at 1568 nm.

## 6. Conclusion

In conclusion, we have demonstrated a stable, high-power, picosecond SPOPO based on MgO:sPPLT, pumped by a Yb-fiber laser at 1  $\mu\text{m}$ , for the first time to our knowledge. The SPOPO is tunable from 1531 to 1642 nm in the signal and 3022-3488 nm in the mid-IR idler, corresponding to a total tuning of 577 nm, with a maximum signal power of 4.23 W at 1593 nm and a maximum idler power of 2.26 W at 3283 nm. By optimizing the SPOPO output coupling, we have obtained as much as 6.28 W of total power at an extraction efficiency of 46.9%. Further, we have demonstrated stable operation close to room temperature, with a passive peak-to-peak power stability of 8.6% for the signal and 8.2% for the idler. The SPOPO provides 17.5 ps signal pulses with time-bandwidth product  $\Delta\nu\Delta\tau\sim 3$ .

## Acknowledgments

This research was supported by the Ministry of Science and Innovation, Spain, through grant TEC2009-07991 and the Consolider project, Science and Application of Ultrafast and Ultraintense Lasers (CSD2007-00013). We also acknowledge partial support by the European Union 7th Framework Program MIRSURG (grant 224042) and the European Office of Aerospace Research and Development (EOARD) through grant FA8655-09-1-3017.